
Article:

Blanquet, E and Williams, PT orcid.org/0000-0003-0401-9326 (2021) Biomass pyrolysis coupled with non-thermal plasma/catalysis for hydrogen production: Influence of biomass components and catalyst properties. Journal of Analytical and Applied Pyrolysis, 159. 105325. ISSN 0165-2370

https://doi.org/10.1016/j.jaap.2021.105325

Biomass pyrolysis coupled with non-thermal plasma/catalysis for hydrogen production: Influence of biomass components and catalyst properties

Ella Blanquet, Paul T. Williams*

School of Chemical and Process Engineering, University of Leeds, Leeds, LS2 9JT, U.K.
(*Corresponding author; Email; p.t.williams@leeds.ac.uk; Tel; #44 1133432504)

ABSTRACT

A novel two-stage pyrolysis-plasma/catalysis process has been developed for hydrogen production from waste biomass. Investigation into; the comparison of the biopolymers, cellulose and lignin; the effect of Mg, Co, Ce, Cu, Fe and Ni as promoter metals added to a Ni-Al_2O_3 catalyst; and the influence of the catalyst support material in relation to hydrogen production was carried out. The combination of plasma and catalysis produced the highest hydrogen and total gas yield from processing waste biomass in comparison to non-plasma pyrolysis-catalysis. The pyrolysis-plasma/catalysis of cellulose produced 4.07 mmol g^{-1} $_{biomass}$ of hydrogen compared with lignin which produced 4.29 mmol g^{-1} $_{biomass}$ of hydrogen. Metal promoters with the Ni-alumina catalyst did not have a strong influence on hydrogen production. However, some catalysts (Cu-Ni-Al_2O_3 and Ni-Ni-Al_2O_3), showed that addition of the metal promoter resulted in a reduced yield of hydrogen. The order of the catalysts in terms of hydrogen yield (H_2 mmol g^{-1} $_{biomass}$) was, Ce-Ni > Co-Ni > Mg-Ni > Fe-Ni > Ni-Ni > Cu-Ni. In addition, different catalyst support materials were investigated. Hydrogen yield was highest with alumina support material compared with titanium oxide and Y-zeolite supports. Hydrogen production was linked to the surface area and porosity, and the dielectric constant of the catalyst material.

Keywords: Biomass; Waste; Pyrolysis; Plasma; Catalyst; Hydrogen

1. Introduction

The European Commission, Energy Strategy has been put in place with the aim of lowering the emissions of greenhouse gases by 40% (based on 1990 levels) together with at least 32% of Europe's energy mix sourced from renewable energy by 2030 [1]. Biomass is a renewable energy which has the advantage of being able to be utilised in several different sectors, as a feedstock for electricity production, heat generation and also biofuels for transport. Biomass is also regarded as carbon neutral in terms of energy supply and the emission of greenhouse gases. The thermochemical conversion of biomass via pyrolysis can produce a bio-oil, char and gas which all have potential for fuel use. However, the bio-oil from biomass pyrolysis is highly oxygenated, acidic and chemically complex, representing properties that restrict its end-use as a liquid fuel [2,3]. Thermochemical processing of biomass via steam, oxygen or air gasification produces a syngas (H_2 + CO), together with lower yields of methane and carbon dioxide [4,5]. Steam gasification increases hydrogen content in the syngas. A recent development has seen the combination of pyrolysis and reforming/gasification processes through the use of two-stage pyrolysis-catalytic steam reforming/gasification reactors that produce high yields of hydrogen-rich syngas [5-9]. The process involves a 1st stage of biomass pyrolysis at ~500 °C then direct catalytic steam reforming/gasification of the product pyrolysis gases/vapours in a closely coupled 2nd stage catalyst reactor operated at a temperature of ~800 °C. The complex hydrocarbons and oxy-hydrocarbons in the gaseous/vapour phase produced during the pyrolysis stage are catalytically steam reformed in the second stage catalyst reactor. In addition to steam reforming of the evolved pyrolysis hydrocarbons, catalytic tar, hydrocarbon and oxy-hydrocarbon cracking may occur and also dry (CO_2) reforming and water gas shift reactions may be involved [8]. The most commonly used catalysts that have been investigated in this process are nickel-based alumina catalysts but have the disadvantage that they are prone to the formation of carbon deposits (coke) on the catalyst and consequent catalyst deactivation [10]. The process conditions of high catalyst reforming temperature of ~800 °C are also a drawback of the process and which may result in catalyst sintering. There has therefore been research to improve the properties of catalysts to minimise coke formation and improve the stability of the catalyst. For example, there has been research into the development of different catalysts and examination of the introduction of metal-promoters which enhance the catalytic activity and improves the stability of the catalysts to thereby improve hydrogen production [6,7].

We have recently reported a further development of the two-stage pyrolysis-catalysis reforming process by replacing the thermal-catalyst reactor with a non-thermal plasma/catalyst reactor [11]. We showed hydrogen could be produced from biomass at the operational catalytic steam reforming temperature of only ~250 °C, rather than the high temperatures of ~800 °C typically used for conventional catalytic steam reforming. However, the yield of hydrogen-rich syngas was low at ~4 mmol $g^{-1}_{biomass}$ compared to conventional thermal catalytic reforming experiments with hydrogen yields typically between 14-25 mmol $g^{-1}_{biomass}$, depending on catalyst composition and process conditions [12-14].

Non-thermal plasma is an interesting process development where the plasma is generated through electricity and involves a large potential difference applied across two electrodes, for example, using a dielectric barrier discharge process (DBD) [15]. The electrical discharge between the two electrodes results in the transformation of the gas between the two electrodes into a plasma with the formation of an intense electric field generating high energy electrons between the discharge gap of the electrodes. The advantage of using non-thermal plasmas to enhance hydrogen yield is that, although the overall gas temperature is low, typically ~200 °C, the plasma contains high energy electrons with high electron energy of 1-10 eV. The electrons interact with the product vapours/gases derived from the biomass pyrolysis gas to produce highly reactive chemical species such as radicals, excited atoms, ions and molecules [16,17]. Additionally, the inclusion of a heterogeneous catalyst into the process (plasma/catalysis), produces a synergy and further promotion of chemical reactions [16-19]. One of the unique properties of plasma-catalyst interaction is that the plasma is formed on the surface and within the pores of the catalyst, enhancing reaction between reactant species and catalyst [17,20,21].

There are few publications on the pyrolysis-plasma/catalysis process for the production of hydrogen from biomass and also on the influence of various process parameters that may increase the overall hydrogen yield. In this work, the pyrolysis-plasma/catalysis process was investigated for hydrogen production from biomass, and the biomass polymers cellulose and lignin using a Ni-Al_2O_3 catalyst. In addition, different metal promoters (Mg, Co, Ce, Cu, Fe and Ni) were added to the Ni-Al_2O_3 catalyst to determine the influence on the yield of hydrogen. Finally, the influence of catalyst support material by comparing Ni-alumina, Ni-titanium oxide and Ni-Y-zeolite was also investigated in terms of hydrogen yield.

2. Materials and methods

2.1. Materials

2.2.1. Biomass

The waste biomass used was in the form of wood pellets provided by Liverpool Wood Pellets Ltd, Liverpool, UK. The particle sample size of the samples used in this work was ~1 mm. Carbon, hydrogen, nitrogen and sulphur analysis (CHNS) of the biomass was analysed with a Thermo EA-2000 instrument. Proximate analysis was undertaken using a Shimadzu – TGA 50 thermogravimetric analyser with a standard temperature programme with a nitrogen purge gas followed by air. The characterisation results for the biomass sample is shown in Table 1.

2.2.2. Catalyst preparation

The catalyst used for the pyrolysis-plasma/catalysis experiments using biomass, cellulose and lignin were carried out using a 5 wt.% Ni-Al_2O_3 catalyst. Further experiments investigated the influence of metal promoters added to the 5 wt.% Ni-Al_2O_3 catalyst to determine the impact on hydrogen generation. In addition, three different catalyst support materials were investigated; alumina, titanium oxide and Y-zeolite each with 5 wt.% nickel. The active metals used to prepare the metal catalyst were obtained from Sigma-Aldrich UK. The support materials, alumina and Y-zeolite were obtained from Nankai University, China and titanium dioxide was obtained from Fischer Scientific Ltd., UK.

The catalyst preparation process used an impregnation method. With 5% weight of Ni and 5 wt.% of promoter, $Ni(NO_3)_2.6H_2O$ and the associated promoter ammonium salt ($Ce(NO_3)_2.6H_2O$, $Cu(NO_3)_2.3H_2O$, $Fe(NO_3)_3.9H_2O$ and $Ni(NO_3)_2.6H_2O$) were dissolved in deionised water. The produced catalysts were therefore, 5 wt.% Mg, Co, Ce, Cu, Fe and Ni added to the 'baseline' 5 wt.% nickel supported on alumina. The addition of 5 wt.% to the 5 wt.% Ni-alumina catalyst thereby produced a 10 wt.% Ni-Al_2O_3 catalyst. The preparation process consisted of dissolution of the metal nitrate with nickel nitrate in deionised water; then the support material (alumina, titanium dioxide or Y-zeolite) was added; the solution was heated by 15 °C increments from ambient temperature to 95 °C to produce a slurry which was dried overnight at 110 °C. Calcination of the catalyst material was undertaken, heating at of 2 °C min^{-1} to a final temperature of 750 °C. The catalyst was then crushed and sieved to a particle size of 1 mm. A consistent particle size was used throughout the work since it has been shown that different catalyst particle sizes can influence the plasma/catalytic process [16]. Catalyst reduction with hydrogen (H_2, 5%; N_2, 95%) was 20 °C min^{-1} to 800 °C, and 1 h at 800 °C. The BET surface area and the BJH porosity of the different catalyst materials was by N_2 adsorption at 77 K, using a Micromeritics TriStar 3000 instrument and the results are shown in Table 2.

2.2. Pyrolysis-plasma/catalysis reactor system

The two-stage biomass pyrolysis-plasma/catalysis experimental reactor system (Figure 1) has been described previously [11,22]. The 1st stage was pyrolysis of the biomass (1 g) in an electrically heated stainless steel reactor. The temperature programme for pyrolysis of the biomass was from 20 °C to 600 °C at 50 °C min^{-1} heating rate followed by 10 mins at 600 °C. The residual char was collected from the sample crucible after each experiment. The biomass pyrolysis gases were passed to a 2nd stage quartz reactor held at a temperature of 250 °C to minimise tar deposition. Nitrogen was used as a carrier gas to transfer the product gases through the reactor system. The 2nd stage involved non-thermal plasma-catalytic steam reforming reactions of the evolved pyrolysis gases with a coaxial Dielectric Barrier Discharge (DBD) plasma. The 1st and 2nd stage reactors were separated by a ceramic insulator tube to prevent electrical discharge. The DBD plasma was generated between a copper mesh outer electrode (80 mm in length) wrapped on the outside of the quartz tube (25 mm o.d. and 22 mm i.d.) and a stainless steel rod inner electrode (18 mm diameter) inside the quartz tube. Thus, the discharge region was ~80 mm with a discharge gap of 2 mm.

The catalyst (1g) was fully packed in the gap (2mm) between the quartz tube and the stainless steel inner rod. Distilled water was inserted into the 2nd stage reactor with a syringe pump to produce steam. Thus, the plasma and catalyst interaction and steam reforming reactions took place in the electrical discharge (plasma) between the two electrodes. Electrical discharge was monitored with a digital oscilloscope. The plasma was generated using a high voltage AC electrical power input of a frequency 1500 Hz and peak voltage of 20 kV maximum. The inner electrode connected to the input power and outer electrode was grounded. A series of dry-ice cooled glass condensers removed the liquid products and the product gases were collected in a 25 L Tedlar™ gas sample bag. The product gases were analysed off-line by packed-column gas chromatography. The hydrocarbon oil and condensed water liquid product was measured by weighing the condensers before and after experimentation. Knowing the mass of input water used for steam generation, the mass of product liquid yield could be determined. Multiple repeat experiments were undertaken with biomass as the feedstock to determine the repeatability of the pyrolysis-plasma/catalysis reactor system at typical reactor conditions; the data produced a standard deviation of 0.43 wt.% for gas yield, 4.3 wt.% for liquid yield (including injected water) and 0.43 wt.% for the gas yield. The reported results in this work represented the mean of at least two experiments.

2.3. Product gas analysis and catalyst carbon determination

The product gases in the Tedlar™ gas sample bag were analysed using three different Varian Ltd., UK, CP-3800 gas chromatographs (GC) as described before [8,11,22]. One GC measured hydrogen, nitrogen, oxygen, carbon monoxide gases, a second measured CO_2 and a third measured C_1 — C_4 hydrocarbons. The mass of each gas was calculated based on the gas concentration, gas flow rate and the ideal gas law.

The carbon deposits formed on the catalyst after the pyrolysis-plasma/catalysis experiments of biomass in relation to different metal promoters was determined by temperature programmed oxidation (TPO) using thermogravimetric analysis (TGA). The TGA was a Shimadzu TGA-50 and used an air atmosphere and the catalyst sample was heated from ambient temperature to 800 °C at 15 °C min^{-1}. The weight loss measured during the oxidation process and in relation to oxidation temperature was used to calculate the mass of carbon on the catalyst.

3. Results and discussion

3.1. Hydrogen yield from biomass, cellulose and lignin

Initial experiments were conducted with the feedstocks of biomass and the biopolymers, cellulose and lignin in relation to the production of hydrogen. Experiments were conducted under three different experimental configurations to ascertain the effect of the non-thermal plasma on hydrogen yield; (i) pyrolysis-catalysis where no plasma was applied to the 2nd stage catalyst reactor but the catalyst was present; (ii) pyrolysis-plasma, where the non-thermal plasma was introduced in the 2nd stage reactor but with no catalyst present; (iii) pyrolysis-plasma/catalysis where non-thermal plasma was used with catalyst in the 2nd stage. The catalyst used throughout was 5 wt.% Ni-Al_2O_3. The experiments used a power input of 40 W which produced a suitable plasma discharge in the 2nd stage plasma reactor and input steam flow rate was 2 g h^{-1}. The results in terms of product yield are shown in Figure 2 and the product gas composition for hydrogen, carbon monoxide, carbon dioxide and methane is shown in Figure 3 for the different experimental configurations. Figure 2 shows that pyrolysis-catalysis of biomass (5 wt.% Ni-Al_2O_3 catalyst but no plasma) produced a gas yield of 10.72 wt.% but increased to 15.63 wt.% when the plasma was introduced to the 2nd stage. This suggests that steam reforming of the pyrolysis hydrocarbons from biomass in the presence of the non-thermal plasma occurred. However, when the 5 wt.% Ni-Al_2O_3 catalyst was added to the pyrolysis-plasma/catalysis process, no discernable increase in the total gas yield occurred. There was also an increase in gas yield for cellulose and lignin as the experimental configuration was changed from pyrolysis-catalysis to pyrolysis-plasma and to pyrolysis-plasma/catalysis; for cellulose, the gas yield was increased from 7.84, to 11.89 and to 12.63 wt.% and for lignin from 6.54, to 7.37 and to 10.13 wt.% respectively. The char yield from biomass was ~10.3 wt.% throughout the experiments since the char yield from pyrolysis of the biomass would be unaffected by the configuration in the downstream 2nd stage. Similarly, the yield of char from pyrolysis of cellulose was ~8.9 wt.% and from lignin was ~22.4 wt.% throughout these experiments.

Figure 3 shows the gas composition from the processing of biomass, cellulose and lignin. The yield of hydrogen from pyrolysis-catalysis of biomass was only 1.13 mmol $g^{-1}{}_{biomass}$, but increased markedly to 3.48 mmol $g^{-1}{}_{biomass}$ for the pyrolysis-plasma process and further increased to 3.94 mmol $g^{-1}{}_{biomass}$ for the pyrolysis-plasma/catalysis process. The processing of cellulose and lignin also showed a clear increase in yield of hydrogenfor example, for cellulose the hydrogen yield increased from 0.81 mmol $g^{-1}{}_{biomass}$ with the pyrolysis-catalysis process to 3.55 mmol $g^{-1}{}_{biomass}$ pyrolysis-plasma process to 4.07 mmol $g^{-1}{}_{biomass}$, with the pyrolysis-plasma/catalysis process. The carbon monoxide yield also increased for the pyrolysis-plasma/catalysis process producing a syngas (H_2 + CO) yield of 7.25 mmol $g^{-1}{}_{biomass}$ for biomass, 7.16 mmol $g^{-1}{}_{biomass}$ for cellulose and 6.15 mmol $g^{-1}{}_{biomass}$ for lignin. Nickel-based catalysts are known for reforming biomass hydrocarbons leading to a higher hydrogen and carbon monoxide gas production [8]. Oxygen was also detected at low levels in the gase produced using the plasma and plasma/catalytic systems. The oxygen is reported to be produced from the plasma induced degradation of CO_2 generated from the biomass pyrolysis [23,24].

It is important to note that the catalytic steam reforming of hydrocarbons (e.g. natural gas) for commercial hydrogen production is for the most part performed at high temperatures of ~800 °C [25]. However, the process conditions of plasma/catalysis in this work was at a much lower temperature of ~250 °C. Therefore, the Ni-Al_2O_3 catalyst used in this work is likely to have low catalytic activity for hydrocarbon reforming. Additionally, other reactions may be occurring in the plasma/catalyst reactor that generate hydrogen from the pyrolysis gases produced from biomass, cellulose or lignin. For example, the water gas-shift reaction involving carbon monoxide and steam to produce hydrogen can occur at temperatures of 200-300 °C [26,27]. In addition, although the operating temperature of the plasma/catalyst reactor was 250 °C, the presence of the plasma reaction environment may induce significantly higher temperatures. Importantly, the catalytic activity of the Ni-Al_2O_3 catalyst may also be enhanced by the plasma interacting with the catalyst surface and within the pores of the catalyst. As suggested by Holzer et al., [28] the increased catalytic activity in plasma/catalysis reactions may be related to hot spots on the surface of the catalyst, due to strong micro-discharges, for example between sharp edges of catalyst particles. These 'hot spots' generating much higher catalyst temperatures than that of the overall gas temperature and thereby promoting catalytic steam reforming. But the micro-size of the discharges and the rapid heat transfer to the pyrolysis gases serves to dissipate the heat and prevent the overall temperature of the catalyst bed to increase [28].

Figure 3 shows that the highest total gas yield and hydrogen yield, were achieved for the pyrolysis-plasma/catalytic experiments. The highly reactive plasma-catalysis environment in relation to catalytic steam reforming for the production of hydrogen may be further explained; Clearly, there is a synergistic relationship between the plasma and catalyst that induces high hydrogen and also high carbon monoxide yields. The reaction environment within the plasma/catalyst zone induces reactions between the plasma, biomass pyrolysis gases and the catalyst surface. The plasma generates highly energetic, high temperature electrons which can degrade the biomass pyrolysis gases and through electron impact, excitation and dissociation reactions, thereby generate of hydrogen [29-31]. In addition, the plasma will interact with the surface of the catalyst, and may alter its electronic and chemical characteristics, for example changing the oxidation state of the catalyst. Synergistically, the catalyst may affect the plasma via enhancing the electric field or discharge type [20]. It has also been reported that the catalyst further increases the temperature of the electron energy and electron temperature, thereby enhancing reactivity [32]. The catalyst also acts as a surface for interaction of the plasma and pyrolysis gases with increased adsorption of reacting species due to the presence of the plasma [16]. The active nickel metal particles in the catalyst will also act as a focus for enhanced selective reforming and cracking reactions. It should also be noted that the interaction of the plasma with the added steam can generate hydrogen from the plasma generated $H^{\bullet}$ and $OH^{\bullet}$ radicals [33].

3.2. Influence of metal promoters to a Ni-alumina catalyst on hydrogen yield

The yield of hydrogen from biomass, cellulose and lignin was low compared to conventional higher temperature catalytic steam reforming, albeit, at significantly lower overall catalyst reforming temperature. Therefore, improvements to the catalytic activity of the Ni-Al_2O_3 catalyst by adding metal promoters was investigated with the aim of increasing hydrogen yield. The affect of metal promoters on overall gas yield and hydrogen yield was studied by adding 5 wt.% Mg, Co, Ce, Cu, Fe and Ni to the 5 wt.% Ni-alumina catalyst. As before, input power was 40 W and steam flow rate 2 g h^{-1}. However, the results (Figure 4) show that there was only a small effect on total gas yield with the addition of the metal promoter to the nickel-alumina catalyst which ranged from 12.27 wt.% (Ni-Ni) to 13.07 wt.% (Fe-Ni). The liquid yield ranged from 67.11 wt.% (Mg-Ni) to 73.91 wt.% (Ni-Ni). In terms of hydrogen yield, Figure 5 shows the gas composition produced from the pyrolysis-plasma/catalysis of the biomass process using the metal-promoted Ni-based catalysts. The catalyst order in regard to hydrogen yield was, Ce-Ni > Co-Ni > Mg-Ni > Fe-Ni > Ni-Ni > Cu-Ni. The hydrogen yield for the 5 wt.% Ni-Alumina catalyst, without a metal promoter, was 3.94 mmol $g^{-1}_{biomass}$ for the pyrolysis-plasma/catalysis of biomass (Figure 3). The addition of cerium as a metal promoter (Ce-Ni-Al_2O_3 catalyst) produced the highest hydrogen yield at 4.22 mmol $g^{-1}_{biomass}$. The advantages of cerium as a metal promoter have been reported before using thermal (non-plasma) processes and have shown enhanced yield of hydrogen from biomass; the cerium acts as an inhibitor for carbon coke formation on the catalyst. Nickel-based catalysts are prone to produce carbon deposits resulting in deactivation. However, the addition of the cerium inhibits coke formation therefore maintaining the reforming activity of the catalyst and enhancing hydrogen yield [10,34-37]. The presence of cerium promotes the reaction of carbon and steam thereby minimising carbon deposition because of its oxygen storage capacity [38]. The addition of cobalt to the nickel-based alumina catalyst produced a hydrogen yield of 4.02 mmol $g^{-1}_{biomass}$ from the pyrolysis-plasma/catalysis of biomass. Cobalt has also been recognised as a metal promoter for nickel-based catalysts for the thermal (non-plasma) catalytic gasification of biomass due to enhancing the activity of the nickel-based catalyst and reducing catalyst coke formation [10]. Youn et al. [39] have also reported that a cobalt-nickel-alumina catalyst showed a significant enhancement of hydrogen yield compared to a nickel-alumina catalyst for the catalytic steam reforming of ethanol for the production of hydrogen. When the Mg modified nickel-alumina catalyst was used (Mg-Ni-Al_2O_3) in the pyrolysis-plasma/catalysis of biomass the hydrogen yield produced was 4.00 mmol g^{-1} $_{biomass}$. The addition of Mg to Ni-Al_2O_3 catalysts has been shown to be an effective promoter for biomass/tar thermal gasification (non-plasma) [10]. The addition of magnesium is reported to enhance the physical strength of the catalyst, minimise sintering and facilitate the adsorption of steam to the surface for steam reforming reactions. The addition of copper to the Ni-alumina catalyst produced a hydrogen yield of 3.58 mmol g^{-1} $_{biomass}$, slightly lower to that achieved without the Cu, whereas Youn et al. [39] observed that the hydrogen yield was significantly higher for Cu-Ni-alumina compared to Ni-alumina. The Ni-Ni-Al_2O_3 catalyst (i.e. 10 wt.% nickel) produced a hydrogen yield of 3.73 mmol $g^{-1}_{biomass}$ for the pyrolysis-plasma/catalysis of biomass, slightly lower than that produced for the 5wt.% Ni-Al_2O_3 catalyst (3.94 mmol $g^{-1}_{biomass}$; Figure 3). The higher amount of nickel may have led to some sintering of the metal particles, resulting in slightly reduced catalytic activity.

Carbon monoxide yield produced from the pyrolysis-plasma/catalysis of biomass was quite similar for all of the metal promoted catalysts, at between 3.09 mmol $g^{-1}_{biomass}$ (Cu-Ni-Al_2O_3) to 3.26 mmol $g^{-1}_{biomass}$ (Co-Ni-Al_2O_3). The yield of carbon dioxide ranged from 3.31 mmol $g^{-1}_{biomass}$ (Ni-Ni-Al_2O_3) to 3.75 mmol $g^{-1}_{biomass}$ (Ce-Ni-Al_2O_3) and methane yield ranged from 0.80 mmol $g^{-1}_{biomass}$ (Cu-Ni-Al_2O_3) to 1.25 mmol $g^{-1}_{biomass}$ (Fe-Ni-Al_2O_3).

There are few reports in the literature on the investigation of different metal-catalysts in the plasma/catalyst process for the production of hydrogen from biomass. Zeng et al. [40] studied different metals (Ni, Co, Cu and Mn) supported on Al_2O_3 for the plasma/catalysis dry reforming of methane. They reported that Ni-Al_2O_3 and Mn/Al_2O_3 catalysts with non-thermal plasma produced a significantly increased conversion of methane. Zeng et al. [41] investigated the influence of metal promoters (K, Ce and Mg) added to a Ni-Al_2O_3 catalyst for the plasma/catalytic reforming of biogas (CH_4 and CO_2). Where addition of all of the promoters enhanced hydrogen production under plasma/catalytic conditions, with the K-Ni-Al_2O_3 catalyst producing the maximum yield of hydrogen. Liu et al. [33] compared Ni-Al_2O_3 and Fe-Al_2O_3 for the plasma/catalytic steam reforming of toluene and showed that Fe-Al_2O_3 produced a higher yield of H_2 and CO i.e. syngas than Ni-Al_2O_3. This was ascribed to the higher oxygen affinity of Fe compared to Ni, thereby Fe-based catalysts increase the surface oxygenated compounds such as, H_2O and O and OH radicals etc during steam reforming reactions. Therefore, hydrogen and carbon monoxide are increased due to steam reforming reactions of the biomass pyrolysis gases and the interaction of radicals with the pyrolysis gases [33].

Figure 6 shows the temperature programmed oxidation (TPO) of the spent catalysts from pyrolysis-plasma/catalysis of biomass with the different metal promoted catalysts. The weight loss shows carbon oxidation reflecting carbon deposits of between 5 wt.% and 7 wt.% of carbon on the used catalyst. Zeng et al. [41] investigated the plasma/catalysis of biogas using different metals (K, Ce and Mg) as promoters on a Ni-Al_2O_3 catalyst. They reported a similar carbon deposition, as found in this work, of 6.54 wt.%, 6.84 wt.% and 6.59 wt.% for Mg-Ni-Al_2O_3, Ce-Ni-Al_2O_3 and K-Ni-Al_2O_3 catalysts respectively.

3.3. Influence of catalyst support material on hydrogen yield

The role of catalyst support material was investigated for the pyrolysis-plasma/catalysis of biomass with the aim of determining the influence on hydrogen production from biomass using the pyrolysis-plasma/catalysis reactor system. The support materials used were alumina, titanium dioxide and Y-zeolite. Alumina is a common support material used for thermal catalytic processes for the production of hydrogen [8]; titanium dioxide, is used in several plasma/catalysis studies [42]; and Y-zeolite, is a catalyst commonly used to crack hydrocarbons [43]. The properties of the support materials investigated are shown in Table 2. Titanium dioxide, Y-zeolite and alumina all had a similar nitrogen adsorption isotherm typical of IUPAC Type IV with Type H2 adsorption-desorption hysteresis representative of highly mesoporous material. Whereas the Y-zeolite had nitrogen adsorption and adsorption-desorption hysteresis characteristics of mesoporosity and microporosity. The BET surface was ~150 m^2 g^{-1} for both alumina and titanium oxide, whereas Y-zeolite had a surface area of 423 m^2 g^{-1}. Y-zeolite had the largest pore size (13.6 nm), followed by titanium oxide (9.5 nm) and alumina had the smallest pore size (3.6 nm). Titanium dioxide had the highest dielectric constant, followed by alumina and Y-zeolite.

Figure 7 shows the product yield from the pyrolysis-plasma/catalysis of biomass in the presence of the Al_2O_3, TiO_2 and Y-zeolite supports and the nickel-based supports with 5 wt.% nickel. The Al_2O_3, support material produced the highest total gas yield at 13.2 wt.% compared to Y-zeolite at 11.9 wt.%. The addition of nickel produced an enhanced gas yield for all of the supported nickel catalysts, at 14.1 wt.% for the Ni-Al_2O_3, 13.3 wt.% for TiO_2 and 13.3 wt.% for Y-zeolite supported catalysts. Although Table 2 shows that the surface area for Al_2O_3 and TiO_2 support materials (~150 m^2 g^{-1}) was significantly lower than for the Y-zeolite support (423 m^2 g^{-1}) and the Y-zeolite contained more micropores, the total gas yield was not significantly different between all the support materials investigated.

Figure 8 shows the gas composition (mmol $g^{-1}{}_{biomass}$) for the pyrolysis-plasma/catalysis of biomass in the presence of the three different support materials and the Ni-based support materials. The hydrogen yield for the Al_2O_3, TiO_2 and Y-zeolite support materials was 3.90 mmol $g^{-1}{}_{biomass}$, 3.26 mmol $g^{-1}{}_{biomass}$ and 3.56 mmol $g^{-1}{}_{biomass}$ respectively. Addition of nickel to the support material produced an increase in hydrogen yield to, 4.06 mmol $g^{-1}{}_{biomass}$, 3.92 mmol $g^{-1}{}_{biomass}$ and 3.75 mmol $g^{-1}{}_{biomass}$ for the Al_2O_3, TiO_2 and Y-zeolite support materials respectively. Therefore, the order of the catalysts for the pyrolysis-plasma/catalysis of biomass in terms of hydrogen yield and syngas (H_2 + CO) yield was Al_2O_3 > Y-zeolite > TiO_2. The production of carbon monoxide was also enhanced by the addition of nickel to the three support materials resulting in a CO yield of 3.21 mmol $g^{-1}{}_{biomass}$, 3.26 mmol $g^{-1}{}_{biomass}$ and 2.66 mmol $g^{-1}{}_{biomass}$ for the Al_2O_3, TiO_2 and Y-zeolite support materials respectively. Therefore, the order of the catalysts for the pyrolysis-plasma/catalysis of biomass in terms of syngas yield was also Ni-Al_2O_3 > Ni-Y-zeolite > Ni-TiO_2.

It has been suggested that porous catalyst support materials within the plasma zone produce an enhanced electric field near the pores which influences the generation of plasma species and also induces micro-discharges inside the pores [20]. Liu et al. [33] reported on the catalytic steam reforming of toluene in a plasma/catalysis system using Ni and Fe active catalyst metals with different catalyst support materials, ZSM-5, Al_2O_3, SiO_2 and CaO. They reported that for the Ni-based catalysts, the highest yield of hydrogen was obtained with Ni-ZSM-5. They also showed that the order of the catalysts in relation to the yield of hydrogen was, Ni-ZSM-5 > Ni-Al_2O_3, > Ni-SiO_2 > Ni-CaO. which was attributed to the direct correlation with surface area of the support materials. The higher surface area providing higher surface area for interaction of active metals and reactants. However, in the work reported here the highest hydrogen yield was produced with Ni-Al_2O_3 which had a markedly lower surface area (155 m^2 g^{-1}) compared with Ni-Y-zeolite with a higher surface area (423 m^2 g^{-1}).

The highest hydrogen yield was obtained with the Ni-Al_2O_3 and Ni-Y-zeolite catalysts which had the lowest dielectric constants compared with the Ni-TiO_2 catalyst. The dielectric constant is a measure of the amount of potential electrical energy, in the form of induced polarization stored in a given volume of a material when an electric field is applied [44]. In plasma/catalysis, the dielectric constant of the support material/catalyst dictates the strength of the electric field and thereby influences the extent of plasma enhancement inside the pores of the catalyst within pores during plasma/catalysis processes [20]. For example, materials such as alumina (Al_2O_3) with lower dielectric constants more easily induce micro-discharges inside catalyst supports compared to materials with higher dielectric constants such as titanium oxide (TiO_2).

Therefore, the results reported here for the hydrogen yield in relation to the different catalyst support materials, suggest that the surface area/porosity of the catalyst and the dielectric characteristics of the support/catalyst both influence hydrogen production. This has also been suggested by Zhang et al. [20] who used a two-dimensional modelling study and reported that both the size of the pores and the dielectric properties of the catalyst support material can influence the plasma generation within the pores of the material. Thereby, the electric field distribution, the plasma species generated inside the catalyst pores and the active catalyst surface available for reactions are all affected.

The highest hydrogen yield achieved in this work using the pyrolysis-plasma/catalysis steam reforming system with the Ni-Al_2O_3 catalyst was 3.94 mmol $g^{-1}_{biomass}$ for biomass, 4.07 mmol $g^{-1}_{biomass}$ for cellulose and 4.29 mmol $g^{-1}_{biomass}$ for lignin. In terms of the metal-promoted catalysts, the highest hydrogen yield from the biomass feedstock was produced with the Ce-Ni-Al_2O_3 catalyst at 4.22 mmol $g^{-1}_{biomass}$ catalyst. Such yields of hydrogen are low compared to the much higher yields of hydrogen for pyrolysis-thermal catalytic (non-plasma) steam reforming reactor systems, where catalysts are used at typical reforming temperatures of ~800 °C

[8,45]. For example, Akubo et al. [8] used a pyrolysis-catalytic steam reforming process, but with a Ni-Al_2O_3 catalyst at 750 °C. They reported a hydrogen yield of 19.7 mmol $g^{-1}_{biomass}$ for the processing of cellulose and 20.5 mmol $g^{-1}_{biomass}$ for lignin. They also investigated the pyrolysis-catalytic reforming of a range of different biomass types and reported hydrogen yields of, for example, 22.1 mmol $g^{-1}_{biomass}$ for coconut shell, 22.9 mmol $g^{-1}_{biomass}$ for sugarcane bagasse, 20.7 mmol $g^{-1}_{biomass}$ for cotton stalk and 16.3 mmol $g^{-1}_{biomass}$ for wheat straw. The high steam reforming temperature of 750 °C - 850 °C used in conventional catalytic steam reforming is the optimum temperature for the Ni-based catalysts typically used. Whereas, the Ni-based catalyst used in this pyrolysis-plasma/catalyst process was 250 °C. Further work using catalysts specifically designed for the low temperature non-thermal plasma environment may enable higher hydrogen yields to be obtained.

4. Conclusions

A two-stage pyrolysis-plasma/catalysis process has been investigated to maximise hydrogen production from biomass at a catalytic reforming temperature of ~250 °C. The introduction of non-thermal plasma via pyrolysis-plasma/catalysis raised both the total gas and hydrogen yields from biomass, cellulose and lignin compared to the pyrolysis-thermal catalysis (non-plasma) process with a Ni-Al_2O_3 catalyst. The pyrolysis-plasma/catalysis of cellulose produced 4.07 mmol $g^{-1}_{biomass}$ of hydrogen and 7.16 mmol $g^{-1}_{biomass}$ of syngas compared with lignin which produced 4.29 mmol $g^{-1}_{biomass}$ of hydrogen and 6.15 mmol $g^{-1}_{biomass}$ of syngas. Introducing promoter metals to the Ni-Al_2O_3 catalyst produced an increase in hydrogen yield for Ce-Ni-Al_2O_3 and Co-Ni-Al_2O_3 catalysts. The order of the catalysts in terms of hydrogen yield (mmol $g^{-1}_{biomass}$) was, Ce-Ni > Co-Ni > Mg-Ni > Fe-Ni > Ni-Ni > Cu-Ni. The Cu-Ni-Al_2O_3 and Ni-Ni-Al_2O_3 catalysts had a negative effect on hydrogen yield from biomass using the pyrolysis-plasma/catalysis process. Different catalyst support materials produced different hydrogen yields, 4.06 mmol $g^{-1}_{biomass}$ for alumina, 3.92 mmol $g^{-1}_{biomass}$ for titanium oxide and 3.75 mmol $g^{-1}_{biomass}$ for Y-zeolite. The hydrogen yield was linked to the dielectric constant of the support material and the influence on plasma development. Also, the surface area and porosity of the support materials also influences the enhancement of plasma intensity, and consequently, the electric field distribution, the plasma induced reactant species inside the pores of the catalyst and the available active catalyst surface for catalytic reactions.

Acknowledgements

We gratefully acknowledge the support of the UK Engineering & Physical Science Research Council (EPSRC) for a research scholarship for EB via the EPSRC Centre for Doctoral Training in Bioenergy (EP/L014912/1).

References

[1] European Commission. Energy Strategy - Clean Energy for all Europeans., European Commission, Brussels, 2019.

[2] Poritosh, R.; Gorrety, D. Prospects for pyrolysis technologies in the bioenergy sector: A review. Renewable and Sustainable Energy Reviews, 77, 59-69, 2017.

[3] Sharifzadeh, M, Sadeqzadeh M., Guo M., Borhani T.N., Konda, N.V.M., Garcia C., Wang L., Hallett J., Shah N. The multi-scale challenges of biomass fast pyrolysis and bio-oil upgrading: Review of the state of the art and future research directions. Progress in Energy and Combustion Science, 71, 1-80, 2019.

[4] Wu C., Williams P.T., Chapter 1: Advanced Thermal Treatment of Wastes for Fuels, Chemicals and Materials Recovery. In, Waste as a Resource, R E Hester & R M Harrison (Editors), RSC, London, pp 1-43, 2013

[5] Pandey B., Prajapati Y.K., Sheth P.N., Recent progress in thermochemical techniques to produce hydrogen gas from biomass: A stste of the art review. International Journal of Hydrogen Energy, 44, 25384-25415, 2019

[6] Chen F., Wu C., Dong L., Jin F., Williams P.T., Huang J. Catalytic steam reforming of volatiles released via pyrolysis of wood sawdust for hydrogen-rich gas production on Fe-Zn/Al_2O_3 nanocatalysts. Fuel, 158, 999-1005, 2015

[7] Jin F.Z., Sun H., Wu, C.F., Ling H.H., Jiang Y.J., Williams P.T., Huang J. Effect of calcium addition on MgAlOx supported Ni catalysts for hydrogen production from pyrolysis-gasification of biomass. Catalysis Today, 309, 2-10, 2018.

[8] Akubo K., Nahil M.A. Williams P.T. Pyrolysis-catalytic steam reforming of agricultural biomass wastes and biomass components for production of hydrogen/syngas. Journal of the Energy Institute, 92(6), 1987-1996, 2019.

[9] Yang S., Chen L., Sun L., Xie X., Zhao B., Si H., Zhang X., Hua D. Novel Ni-Al nanosheet catalyst with homogeneously embedded nickel nanoparticles for hydrogen-rich syngas production from biomass pyrolysis. International Journal of Hydrogen Energy, 46, 1762-1776, 2021

[10] Wu C, Williams P.T. Nickel-based catalysts for tar reduction in biomass gasification. Biofuels 2 451–64, 2011.

[11] Blanquet E. Nahil M. Williams P.T. Enhanced hydrogen-rich gas production from waste biomass using pyrolysis with non-thermal plasma-catalysis. Catalysis Today, 337, 216-224, 2019.

[12] Wu C., Wang L.Z., Williams P.T., Shi J., Huang J. ‘Hydrogen production from biomass gasification with Ni/MCM-41 catalysts: Influence of Ni Content.’ Applied Catalysis B: Environmental, 108, 6-13, 2011.

[13] Nahil M.A., Wang X., Wu C., Yang H., Chen H., Williams P.T., Novel bi-functional Ni–Mg–Al–CaO catalyst for catalytic gasification of biomass for hydrogen production with in situ CO_2 adsorption. Royal Society of Chemistry, Advances, 3, 5583-5590, 2013.

[14] Wu C., Wang Z., Wang L., Huang J., Williams P.T. Catalytic steam gasification of

biomass for a sustainable hydrogen future: Influence of catalyst composition. Waste & Biomass Valorisation, 5, 175-180, 2014.

[15] Gao X. Lin Z., Li T., Huang L., Zhang J., Askari S., Dewangan N., Jangam A., Kawi S., Recent developments in dilectric barrier discharge plasma-assisted catalytic dry reforming of methane over Ni-based catalysts. Catalysts, 11, 455, 2021

[16] Whitehead J.C., Plasma-catalysis: the known knowns, the known unknowns and the unknown unknowns. Journal of Physics: Applied Physics, 49, 243001, 2016

[17] Chung W.C., Mei D.H., Tu X., Chang M.B., Removal of VOCs from gas streams via plasma and catalysis. Catalysis Reviews, 61(2) 270-331, 2019.

[18] Liu L., Zhang Z., das S., Kawi S., Reforming of tar from biomass gasification in a hybrid catalysis-plasma system: A review. Applied Catalysis B: Environmental, 250, 250-272, 2019.

[19] Xiao K.M., Li X.C., Santoso J., Wang H.R., Zhang K., Wu J., Zhang D.K., Synergistic effect of dielectric barrier discharge plasma and Mn catalyst on CO reforming of toluene. Fuel, 285, Article Number 119057, 2021

[20] Zhang Y.R., Neyts E.C., Bogaerts A. Influence of the material dielectric constant on plasma generation inside catalyst pores. Journal Physical Chemistry, 120, 25923-25934, 2016.

[21] Mei D.H., Ashford B., He Y.L., Tu X., Plasma-catalytic reforming of biogas over supported Ni catalysts in a dielectric barrier discharge reactor: Effect of catalyst supports. Plasma Process. Polym. 14, 1-13, 2017.

[22] Aminu I., Nahil M.A. Williams P.T. Hydrogen from waste plastics by two-stage pyrolysis/low temperature plasma catalytic processing. Energy & Fuels, 34(9), 11679-11689, 2020.

[23] Brock, S.L., Shimojo, T., Marquez, M., Marun, C., Suib, S.L., Matsumoto, H. and Hayashi, Y. 1999. Factors influencing the decomposition of co_2 in ac fan-type plasma reactors: frequency, waveform, and concentration effects. Journal of Catalysis**.** 184(1), 123–133, 1999.

[24] Zheng, G., Jiang, J., Wu, Y., Zhang, R. and Hou, H. The mutual conversion of CO_2 and CO in dielectric barrier Discharge (DBD). Plasma Chemistry and Plasma Processing. 23(1), 59–68, 2003.

[25] Czernik, S., French, R., Feik, C. and Chornet, E. Biomass thermoconversion processes. Industrial & Engineering Chemistry Research. 41, 4209–4215, 2002.

[26] Hilaire, S., Wang, X., Luo, T., Gorte, R.J. and Wagner, J. A comparative study of water-gas-shift reaction over ceria-supported metallic catalysts. Applied Catalysis A: General. 258(2), 271–276, 2004.

[27] Smith, B. A review of the water gas shift reaction kinetics. International Journal of Chemical Reactor Engineering. 8(R4), 1–32, 2010.

[28] Holzer, F., Kopinke, F.D. and Roland, U. Influence of ferroelectric materials and catalysts on the performance of Non-Thermal Plasma (NTP) for the removal of

air pollutants. Plasma Chemistry and Plasma Processing. 25(6), pp.595–611, 2005.

[29] Freidman, A., Plasma Chemistry. 2008, New York: Cambridge University Press.

[30] Chung, W.C., Chang M., Review of catalysis and plasma performance on dry reforming of CH4 and possible synergistic effects. Renewable Sustainable Energy Reviews, 62, 13-31, 2016

[31] Mehta, P., Barboun P., Go D.B., Hicks J.C., Schneider W.F., Catalysis enabled by plasma activation of strong chemical bonds: A review. ACS Energ. Lett. 4, 1115−1133, 2019.

[32] Wang, L., Yi Y., Wu C., Guo H., Tu X., One-step reforming of CO_2 and CH_4 to high-value liquid chemicals and fuels at room temperature by plasma-driven catalysis. Angew. Chem. Intl. Ed., 56, 13679-13683, 2017.

[33] Liu, L., Wang Q., Song J., Ahmad S., Yang X., Sun Y., Plasma-assisted catalytic reforming of toluene to hydrogen rich syngas. *Catal. Sci. Technol.,* **7**(18), 4216-4231, 2017.

[34] Fu P, Yi W, Li Z, Bai X, Zhang A, Li Y, Li Z. Investigation on hydrogen production by catalytic steam reforming of maize stalk fast pyrolysis bio-oil. International Journal of Hydrogen Energy, 39, 13962–13971, 2014.

[35] Kimura T., Miyazawa T., Nishikawa J, Kado S., Okumura K., Miyao T., Naito S., Kunimori K., Tomishige K. Development of Ni catalysts for tar removal by steam gasification of biomass. Applied Catalysis B-Environmental, 68, 160-170, 2006

[36] Buffini N.I., Pompeo F., Santori G.F., Nichio N.N., Nickel catalyst applied in steam reforming of glycerol for hydrogen production. Catalyst Communications, 10, 1656-1660, 2009.

[37] Tomishige K., Kimura T., Nishikawa J., Miyazawa T., Kunimori K Promoting effect of the interaction between Ni and CeO on steam gasification of biomass. Catalyst Communications, 8, 1074-1079, 2007.

[38] Miyazawa T., Kimura T., Nishikawa J., Kado S., Kunimori K., Tomishige K. Catalytic performance of supported Ni catalysts in partial oxidation and steam reforming of tar derived from the pyrolysis of wood biomass. Catalysis Today, 115, 254-262, 2006.

[39] Youn M.H., Seo J.G., Kim P., Kim J.J., Lee H.I. Song I.K. Hydrogen production by autothermal reforming of ethanol over Ni/Y-Al_2O_3 catalysts: Effect of second metal addition. Journal of Power Resources, 162, 1270-1274, 2006.

[40] Zeng Y., Zhu X., Mei D., Ashford B., Tu X. Plasma-catalytic dry reforming of methane over γ-Al_2O_3 supported metal catalysts. Catalysis Today, 256, 80-87, 2015

[41] Zeng Y.X., Wang L., Wu C., Wang J.Q., Shen B.X., Tu X. Low temperature reforming of biogass over K-, Mg- and Ce-promoted Ni-Al O catalysts for the production of hydrogen rich syngas: Understanding the plasma-catalytic synergy. Applied Catalysis B: Environmental, 224, 469-478, 2018.

[42] Fan Y.S., Zhu M.F., Jin L.Z., Cui E.T., Zhu L., Cai Y.X., Zhao W.D., Catalytic upgrading of biomass-derived vapors to bio-fuels via modified HZSM-5 coupled with DBD: Effects of different titanium sources. Renewable Energy, 157, 100-115, 2020.

[43] Williams P.T. and Horne P.A. The influence of catalyst type on the composition of upgraded biomass pyrolysis oils. Journal of Analytical & Applied Pyrolysis 31, 39-61, 1995.

[44] Ilic J. Wood: Electrical properties, in Mahajan S. Encyclopedia of Materials: Science and Technology, Pergamon, Oxford, UK, 2001.

[45] Wu, C, Williams, PT, Wang, Z, Huang, J. Pyrolysis/gasification of cellulose, hemicellulose and lignin for hydrogen production in the presence of various nickel-based catalysts. Fuel. 106, 697–706, 2013.

Table 1. Proximate and ultimate analysis of the biomass sample (as received).

Proximate Analysis (wt.%)		Ultimate analysis (wt.%)	
Moisture	7.77	Carbon	46.07
Volatiles	86.43	Hydrogen	4.97
Fixed carbon	5.50	Nitrogen	0.12
Ash	0.30	Sulphur	0.00
		Oxygen	40.77[a]

[a] By difference

Table 2. Surface area and porosity characteristics and dielectric constant of the catalyst support materials

	Alumina	**Titanium oxide**	**Y-zeolite**
Isotherm type	Type IV	Type IV	Type IV
Hysteresis type	H2 (highly mesoporous)	H2 (highly mesoporous)	H3 (mesopores & micropores)
BET surface area (m^2 g^{-1})	155	151	423
Average BJH pore volume (cc g^{-1})	0.404	0.454	0.251
Average BJH pore size (nm)	3.598	9.490	13.661
Dielectric constant[a]	8 – 11	40 – 100	1.5 – 5

[a] [20]

FIGURE CAPTIONS

Figure 1. Schematic diagram of the experimental pyrolysis-plasma/catalytic reactor system

Figure 2. Product yield for (a) Pyrolysis-Catalysis, (b) Pyrolysis-Plasma, (c) Pyrolysis-plasma/catalysis of biomass cellulose and lignin

Figure 3. Gas composition for (a) Pyrolysis-Catalysis, (b) Pyrolysis-Plasma, (c) Pyrolysis-plasma/catalysis of biomass cellulose and lignin

Figure 4. Product yield in relation to different metal promoters applied to Ni-Al_2O_3 catalyst from the pyrolysis-catalytic non-thermal plasma steam reforming of biomass

Figure 5. Effect of metal promoters applied to Ni-Al_2O_3 catalyst on the composition of the product gas in relation to the pyrolysis, plasma-catalysis of biomass.

Figure 6. Effect of metal promoters on coke deposition on the catalyst after pyrolysis, plasma-catalysis of biomass in relation to different metal promoters

Figure 7. Influence of catalyst support material and support material with 5 wt.% nickel in relation to the product yield from the pyrolysis, plasma-catalysis of biomass

Figure 8. Influence of catalyst support material and support material with 5 wt.% nickel in relation to the gas composition from the pyrolysis, plasma-catalysis of biomass

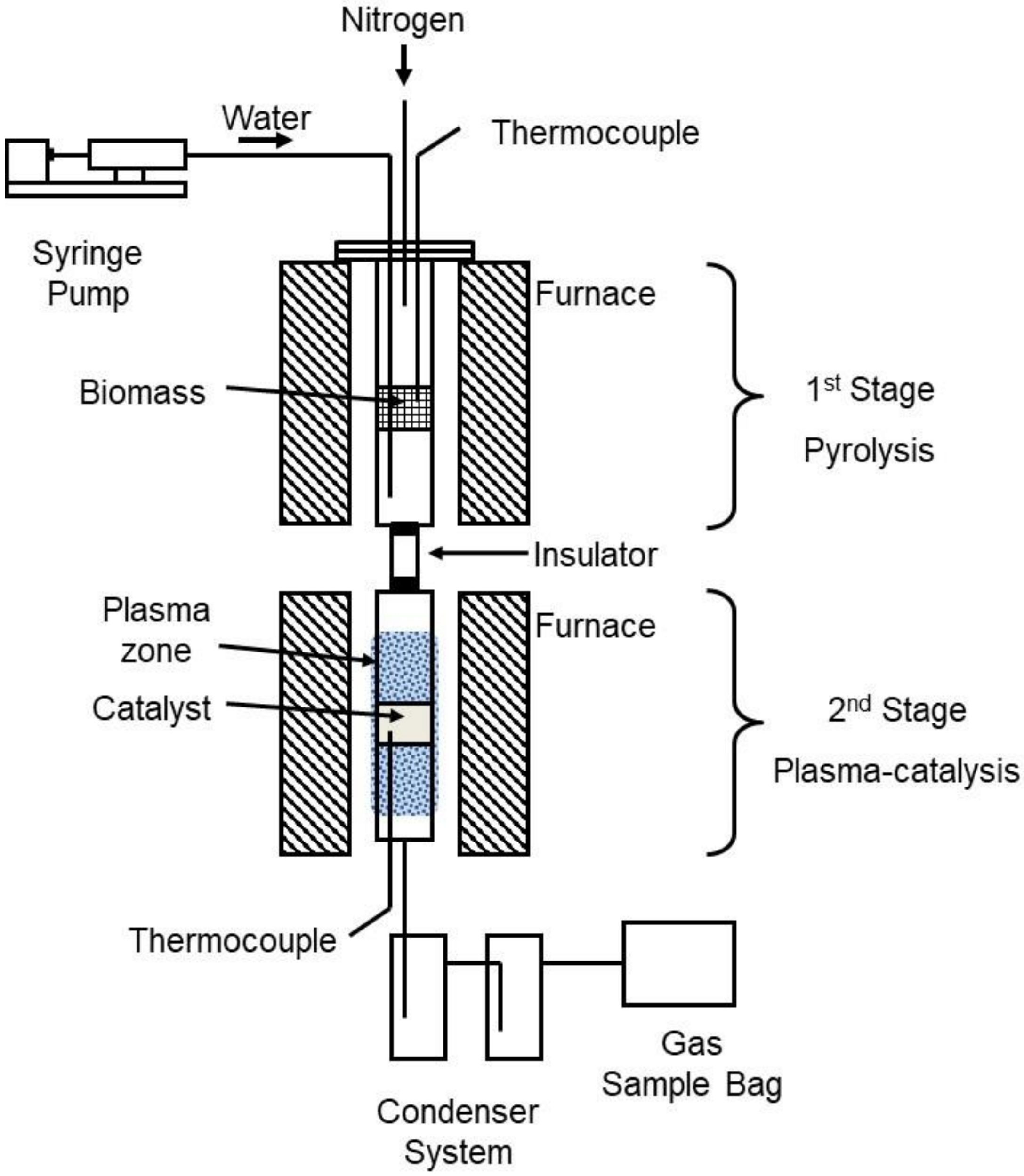

Figure 1. Schematic diagram of the experimental pyrolysis-plasma/catalytic reactor system

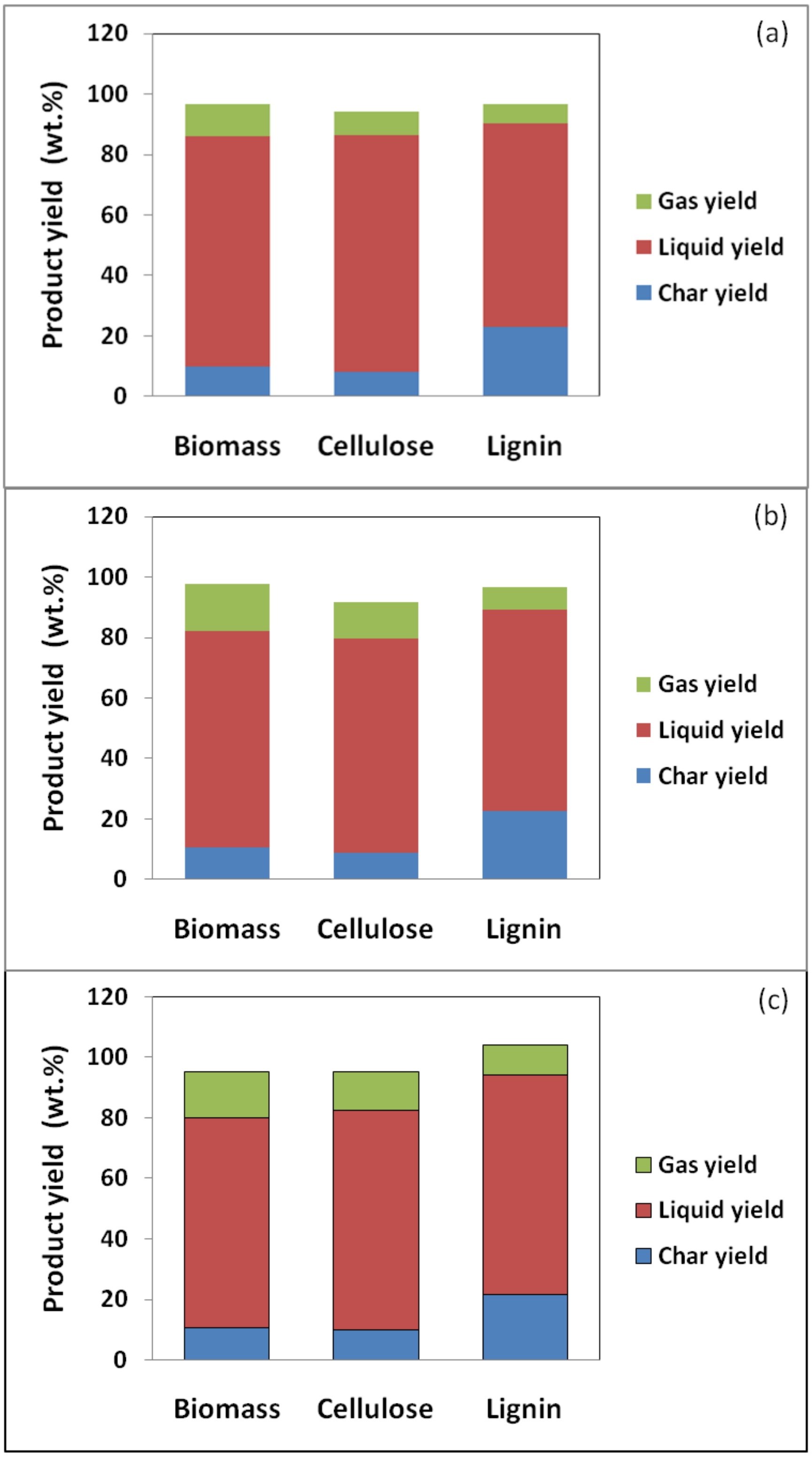

Figure 2. Product yield for (a) Pyrolysis-Catalysis, (b) Pyrolysis-Plasma, (c) Pyrolysis-plasma/catalysis of biomass cellulose and lignin

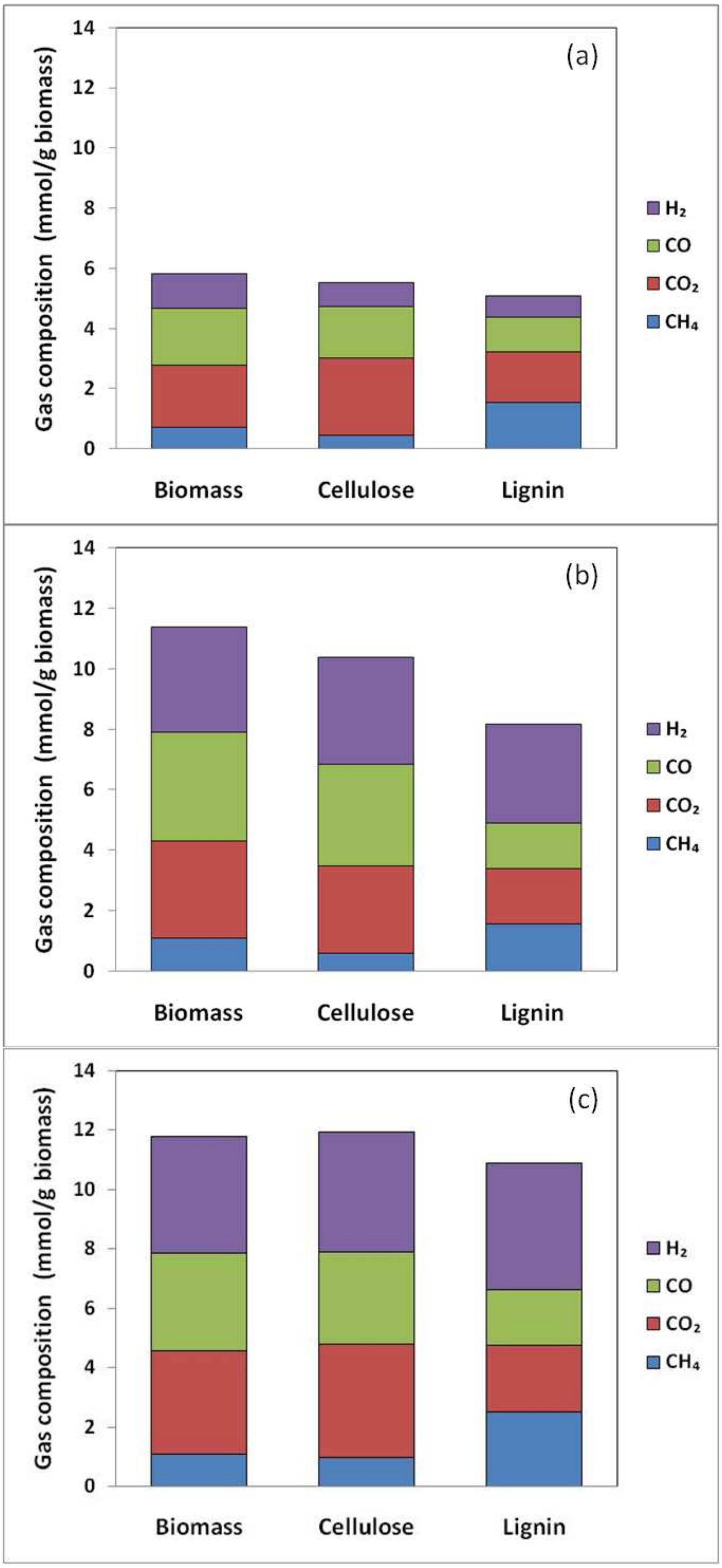

Figure 3. Gas composition for (a) Pyrolysis-Catalysis, (b) Pyrolysis-Plasma, (c) Pyrolysis-plasma/catalysis of biomass, cellulose and lignin

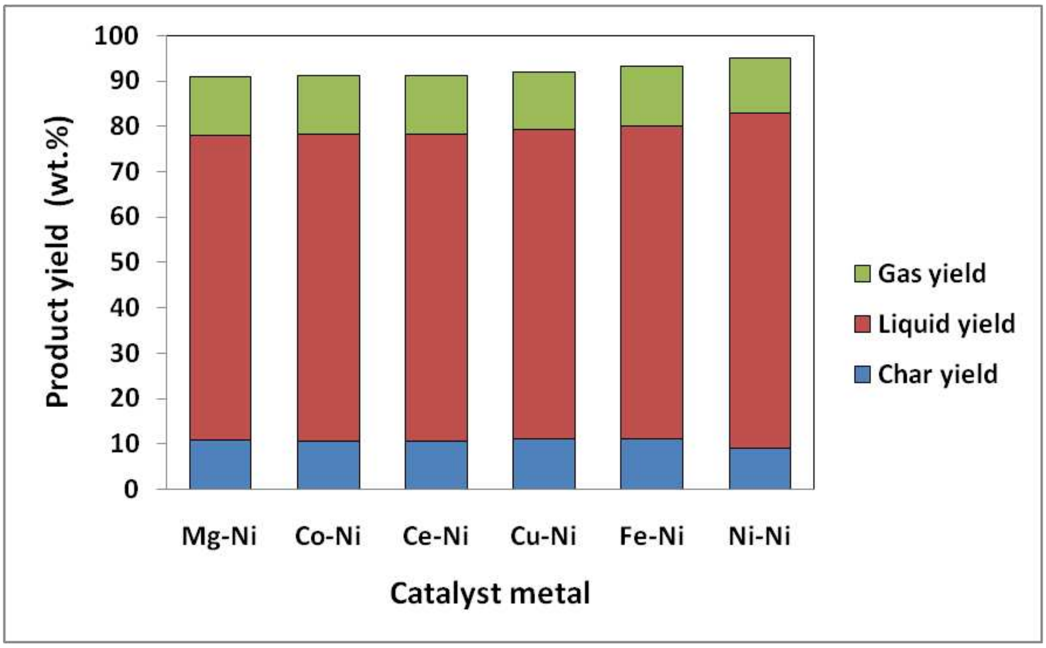

Figure 4. Product yield in relation to different metal promoters applied to Ni-Al_2O_3 catalyst from the pyrolysis-catalytic non-thermal plasma steam reforming of biomass

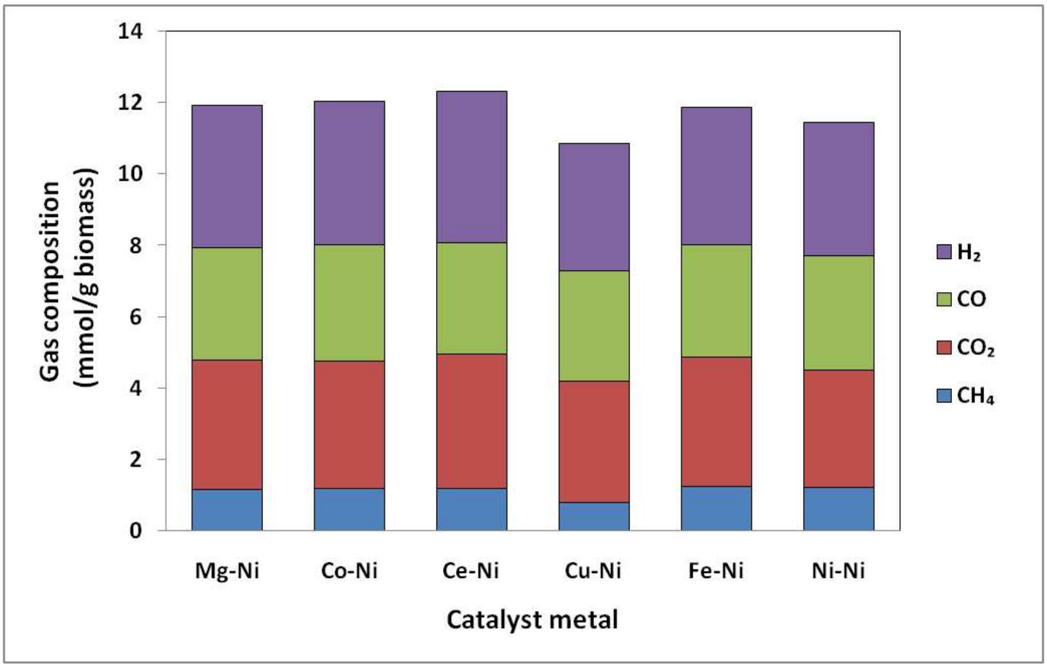

Figure 5. Effect of metal promoters applied to Ni-Al_2O_3 catalyst on the composition of the product gas in relation to the pyrolysis, plasma-catalysis of biomass.

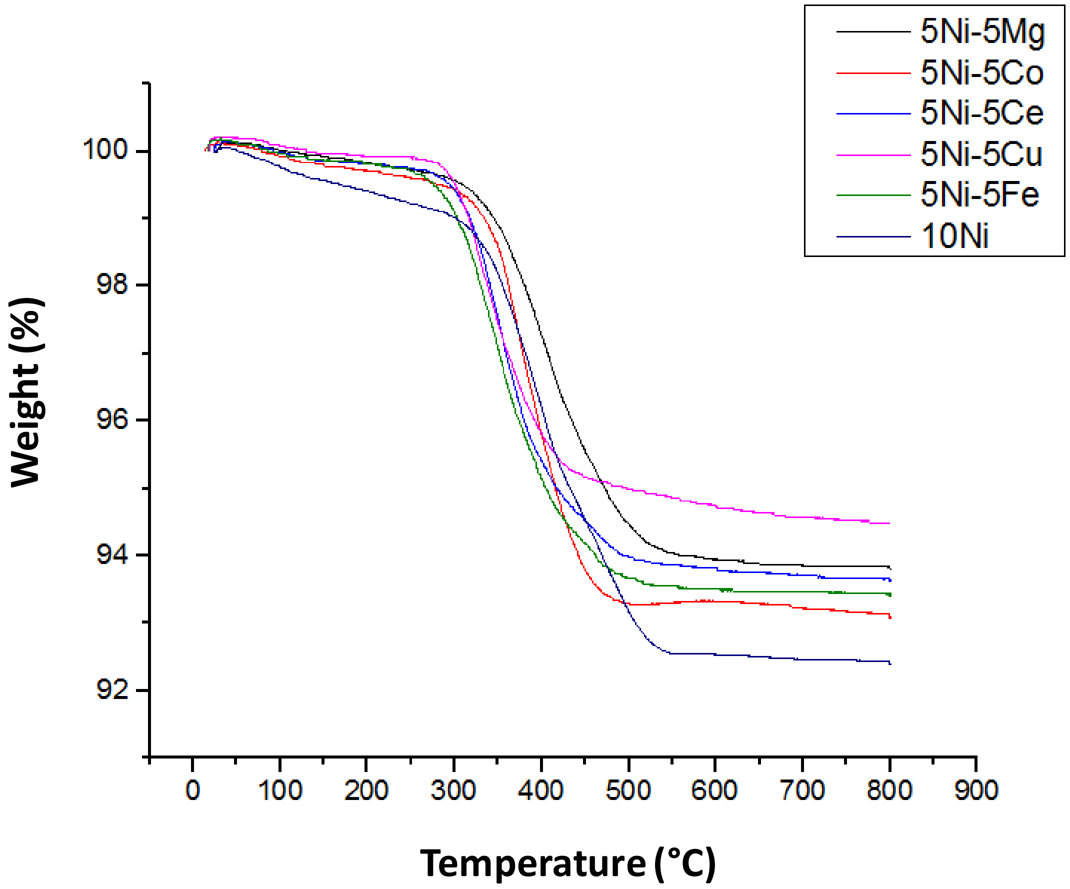

Figure 6. Effect of metal promoters on coke deposition on the catalyst after pyrolysis, plasma-catalysis of biomass in relation to different metal promoters.

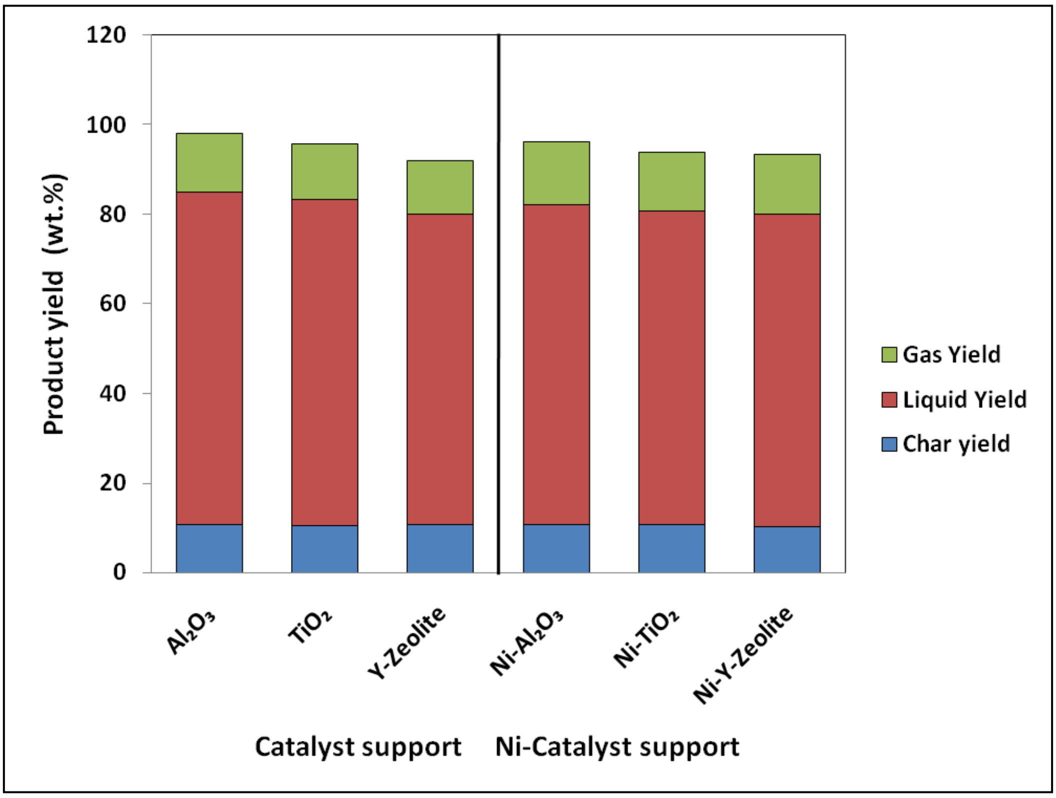

Figure 7. Influence of catalyst support material and support material with 5 wt.% nickel in relation to the product yield from the pyrolysis, plasma-catalysis of biomass

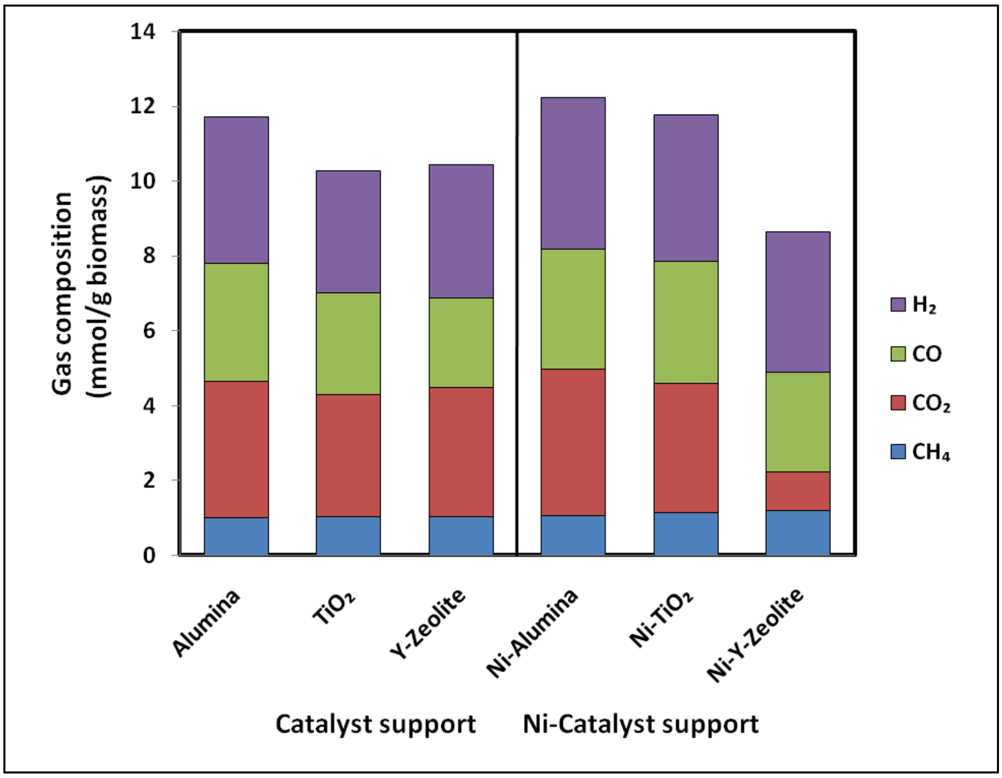

Figure 8. Influence of catalyst support material and support material with 5 wt.% nickel in relation to the gas composition from the pyrolysis, plasma-catalysis of biomass